Pediatric Radiology (2018) 48:1307–1323
https://doi.org/10.1007/s00247-018-4123-y

PEDIATRIC BODY MRI

Thoracoabdominal imaging of tuberous sclerosis

Cara E. Morin[1] · Nicholas P. Morin[2] · David N. Franz[3] · Darcy A. Krueger[3] · Andrew T. Trout[1] · Alexander J. Towbin[1]

Received: 14 December 2017 / Revised: 2 February 2018 / Accepted: 19 March 2018

Abstract
Imaging of tuberous sclerosis complex has rapidly evolved over the last decade in association with increased understanding of the disease process and new treatment modalities. Tuberous sclerosis complex is best known for the neurological symptoms and the associated neuroimaging findings, and children with tuberous sclerosis complex require active surveillance of associated abnormalities in the chest, abdomen and pelvis. Common findings that require regular imaging surveillance are angiomyolipomas in the kidneys and lymphangioleiomyomatosis in the chest. However multiple rarer associations have been attributed to tuberous sclerosis complex and should be considered by radiologists reviewing any imaging in these children. In this review the authors discuss the spectrum of imaging findings in people with tuberous sclerosis complex, focusing on MR imaging findings in the chest, abdomen and pelvis.

Keywords Angiomyolipoma · Children · Magnetic resonance imaging · Tuberous sclerosis complex

Introduction

Tuberous sclerosis complex (TSC) is an autosomal-dominant genetic disease with a variable phenotype characterized by the formation of tumors in multiple organs. The most commonly involved organs are the brain, skin, kidney, lung and heart, with most morbidity and mortality stemming from the neurologic, pulmonary and renal manifestations of the disease. Early descriptions of TSC date to 1862 and refer to a child with cardiac tumors and multiple scleroses in the brain [1]. Similar associations soon broadened to include cardiac and renal tumors and characteristic skin lesions. The genes responsible for TSC, *TSC1* and *TSC2,* were identified in the 1990s [2]. The first International TSC Consensus Conference put forth diagnostic criteria for TSC in 1998 [3]. These criteria were updated in 2012 and included genetic criteria with identification of pathogenic *TSC1* or *TSC2* mutations being sufficient for diagnosis (Table 1) [1].

✉ Alexander J. Towbin
alexander.towbin@cchmc.org

[1] Department of Radiology,
Cincinnati Children's Hospital Medical Center,
3333 Burnet Ave., MLC 5031, Cincinnati, OH 45229, USA

[2] Division of Emergency Medicine,
Cincinnati Children's Hospital Medical Center,
Cincinnati, OH, USA

[3] Division of Neurology,
Cincinnati Children's Hospital Medical Center,
Cincinnati, OH, USA

Neurologic and dermatologic findings in TSC

The clinical presentation of TSC is quite varied even within families sharing the same mutation. TSC has a population prevalence of 1 in 20,000 and an incidence of 1/6,000 to 1/10,000 live births [4, 5]. Seizures are the most common presenting feature of TSC. Epilepsy occurs in 85–96% of people with TSC, typically manifesting as focal seizures or infantile spasms beginning within the first few months of age through 3 years of age [6]. Neuroanatomical findings of TSC include cerebral cortical tubers, subependymal nodules and subependymal giant cell astrocytomas [7]. Ninety percent of individuals with TSC have some form of neurocognitive dysfunction, termed TSC-associated neuropsychiatric disorders by the 2012 consensus conference, including autism spectrum disorders, intellectual disabilities, psychiatric disorders, and neuropsychological deficits as well as school and occupational difficulties [1].

The most common dermatologic manifestation in TSC is hypomelanotic macules. Also called "ash leaf spots," these lesions are identified in 90% of people with TSC and are typically seen at birth or during early infancy [8, 9]. Facial angiofibromas are hamartomatous nodules of vascular and connective tissue present in 75% of people with TSC with onset usually by 5 years of age. Other common cutaneous

Table 1 Clinical diagnostic criteria from the 2012 International Tuberous Sclerosis Complex Consensus Conference (used with permission [1])

Major features	Minor features
Hypomelanotic macules (≥3, at least 5-mm diameter)	"Confetti" skin lesions
Angiofibromas (≥3) or fibrous cephalic plaque	Dental enamel pits (>3)
Ungual fibromas (≥2)	Intraoral fibromas (≥2)
Shagreen patch	Retinal achromic patch
Multiple retinal hamartomas	Multiple renal cysts
Cortical dysplasias[a]	Nonrenal hamartomas
Subependymal nodules	
Subependymal giant cell astrocytoma	
Cardiac rhabdomyoma	
Lymphangioleiomyomatosis (LAM)[b]	
Angiomyolipomas (≥2)[b]	

TSC1 or *TSC2* mutation in deoxyribonucleic acid (DNA) from normal tissues is sufficient to make the diagnosis without these criteria. Note, however, that 10–25% of patients with TSC do not have a gene defect. **Definite diagnosis** includes two major features or one major feature with ≥2 minor features. **Possible diagnosis** includes either one major feature or ≥2 minor features

[a] Includes tubers and cerebral white matter radial migration lines

[b] A combination of the two major clinical features (LAM and angiomyolipomas) without other features does not meet criteria for a definite diagnosis

findings include fibrous cephalic plaques (25% of patients), ungual fibromas (increasing frequency with age to 80%), shagreen patches (50%) and confetti skin lesions (3–58%) [8–10].

Genetics and therapies in TSC

While TSC is heritable, two-thirds of people with TSC have spontaneous mutations [11, 12]. *TSC1* and *TSC2* encode for the proteins hamartin and tuberin, respectively. These proteins are part of a heteromeric complex that negatively regulates cell growth and proliferation through inhibition of the mechanistic target of rapamycin complex 1 (mTORC1). Pathogenic mutations in either *TSC1* or *TSC2* lead to loss of function and constitutive activation of mTORC1 and resultant tumor formation [2].

Historically, TSC treatment involved symptomatic therapy with anti-epileptic drugs and surgical tumor removal. Since the discovery of the TSC genes there has been considerable interest and study of mTOR inhibitors for use in TSC. Two randomized controlled trials, EXIST-1 and EXIST-2, showed efficacy in reducing size of TSC-associated subependymal giant cell astrocytomas (SEGA) and renal angiomyolipomas [13, 14]; as a result, everolimus was approved by the U.S. Food and Drug Administration to treat SEGA in 2010 and renal angiomyolipomas in 2012. Other studies have shown promise in treating seizures in TSC with everolimus. A prospective study of refractory epilepsy in people with TSC reported seizure frequency reduction of 50% in 12 of 20 patients [15], which more recently was confirmed with a randomized multicenter phase III clinical trial (EXIST-3) [16, 17]. Treatment with mTOR inhibitors has also been shown to reduce renal cyst burden and facial angiofibromas in TSC [18, 19].

Thoracoabdominal imaging recommendations/surveillance guidelines

Per the 2012 International Tuberous Sclerosis Complex Consensus Conference, a baseline abdominal MRI is recommended for all people who are newly diagnosed with TSC to evaluate for renal angiomyolipomas (AMLs) and cysts (among other findings discussed later in this paper) [1, 20]. Abdominal CT or renal ultrasound might be considered when MRI is unavailable or contraindicated, but these are associated with increased radiation exposure (in the case of CT) or reduced ability to identify lipid-poor AML (in the case of renal ultrasound) [20, 21].

In addition, a baseline chest CT is recommended to evaluate for lymphangioleiomyomatosis (LAM) in any person with pulmonary symptoms or in asymptomatic women older than 18 years of age. Subsequently, it is recommended that people with TSC receive an abdominal MRI every 1–3 years (focused on the kidneys). Adults with TSC should be screened with chest CT every 5–10 years or every 2–3 years if previously diagnosed with LAM. In the case of new clinical symptoms or lab abnormalities, targeted imaging should be obtained as appropriate.

Thoracoabdominal MR imaging protocols

Screening abdominal MRI can generally be performed without intravenous contrast screening exam. The protocol utilized at our institution is outlined in Table 2 and includes a

Table 2 Abdominal MRI protocol at authors' institution

Sequence	Plane(s)
T2-weighted turbo/fast spin echo	Coronal, axial
T1-weighted turbo/fast spin echo	Coronal
T2-weighted turbo/fast spin echo with fat saturation	Axial
Dixon GRE (including in-phase, opposed-phase, fat, and water images) multiphase (or chemical shift)	Axial

GRE gradient recalled echo, *MRI* magnetic resonance imaging

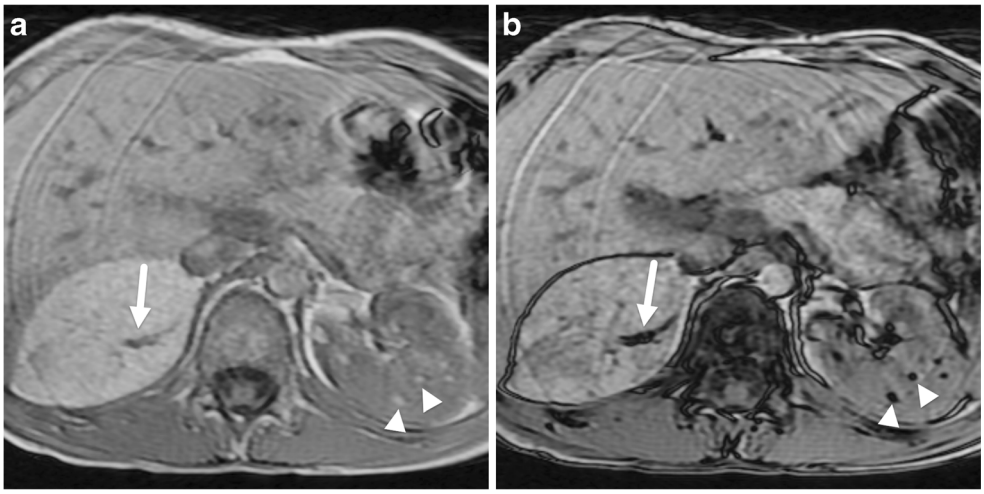

Fig. 1 Tuberous sclerosis complex and a large adrenal angiomyolipoma (AML) in a 12-year-old boy. **a, b** Axial MRI. **a** In-phase and (**b**) opposed-phase images show mild signal dropout within the adrenal lesion on the opposed-phase image. The signal dropout is most concentrated around the intratumoral vessel (*arrow*). Signal dropout is also present in the multiple small left renal AMLs (*arrowheads*)

combination of coronal and axial T1-weighted, T2-weighted and multipoint Dixon gradient recalled echo (GRE) sequences (including in-phase, opposed-phase, fat and water images). Chemical shift imaging (in- and opposed-phase) could be substituted when multipoint Dixon is not available. Intravenous contrast agent is not necessary because it does not provide increased sensitivity for evaluating AMLs vs. renal cell carcinoma [22].

Thoracoabdominal imaging findings

Angiomyolipomas

Angiomyolipomas (AMLs) are benign tumors composed of mature adipose tissue, dysmorphic blood vessels, and smooth muscle [23–25]. Initially described as hamartomatous lesions, AMLs are now considered part of the perivascular epithelioid family of tumors. Two histological types of AMLs are recognized: a classic type and an epithelioid variant. The epithelioid variant is very rare, shows almost exclusively epithelioid morphology, and can be more aggressive in behavior compared to the classic type [23, 24, 26].

AMLs can occur in multiple organs in the abdomen including the liver, pancreas, spleen, adrenal glands, mesentery and kidneys (Figs. 1 and 2) [27–31]. Hepatic AMLs have been reported in up to 13% of pediatric patients with TSC and are commonly multiple and usually seen in people with bilateral diffuse renal AMLs [27, 28]. Renal AMLs are present in up to 80% of pediatric patients with TSC and these children frequently have multiple lesions in both kidneys. Two or more angiomyolipomas are considered to be one of the major features in the clinical diagnostic criteria for TSC [1]. Children with renal AMLs are at risk of spontaneous tumoral hemorrhage and renal failure [32]. Complications of AMLs, includ-

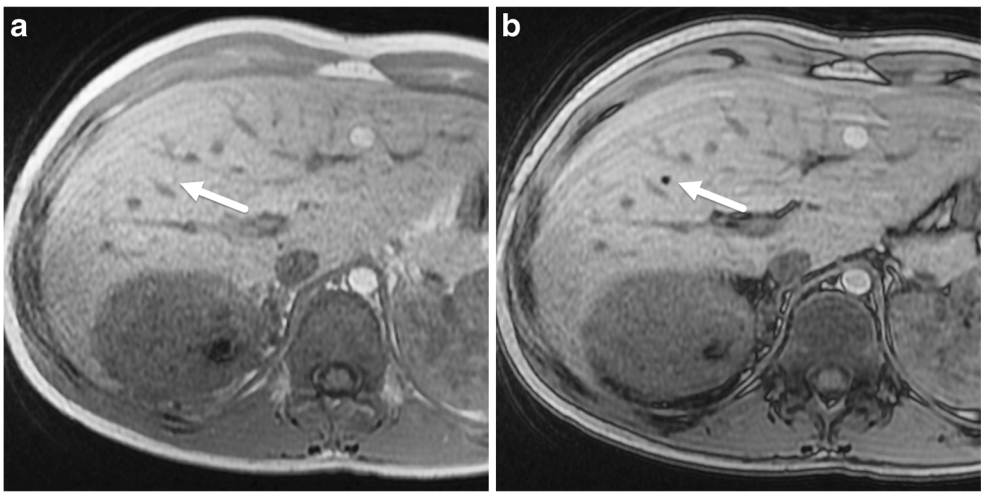

Fig. 2 Tuberous sclerosis complex with a hepatic angiomyolipoma (AML) in an 11-year-old boy. **a, b** Axial MRI. **a** In-phase and (**b**) opposed-phase images show a small hepatic AML (*arrow*) in segment 5 of the liver. The lesion is slightly hyperintense compared to the liver on the in-phase image and has diffuse signal dropout on the opposed-phase image. Note that both images demonstrate aortic pulsation artifact with a pseudo-lesion in the left hepatic lobe anterior to the aorta

ing spontaneous rupture and hemorrhage, are more likely to occur in tumors larger than 4 cm and in tumors with aneurysms larger than 5 mm (Fig. 3) [25, 33–36]. Complications from renal lesions, including hemorrhage and renal failure, are the leading cause of death in adults with TSC [34, 37].

AMLs can be quite variable in appearance, with macroscopic fat-containing and microscopic fat-containing and lipid-poor AMLs all known to occur. The fat-containing lesions are easy to identify on both fat-saturated images and opposed-phase images because of the loss of signal (Fig. 4). AMLs with macroscopic fat can also be identified by the "India ink artifact" on opposed-phase imaging. Because the lesions contain variable proportions of dysmorphic blood vessels and smooth muscle, the lesions are often heterogeneous. Intralesional vessels can be identified as hypointense structures on T2-weighted fat-saturated images while the smooth muscle component is of intermediate signal intensity. It should be noted that while most AMLs are discrete lesions, they can also have an infiltrative pattern and completely replace the normal renal parenchyma (Fig. 5).

AMLs have a variable appearance on opposed-phase imaging. Smaller lesions have complete signal drop-out because fat and water are entirely contained in the same voxel (Fig. 4). Larger AMLs have a different appearance, with a peripheral border of signal drop-out as well as linear septations of signal drop-out representing the interface between the adipose tissue and smooth muscle (Fig. 1).

Fat-poor AMLs (classic variants with low 4% or less fat content on histology) [25, 26] generally appear hypointense on both T1- and T2-weighted imaging (Fig. 6). These lesions do not have appreciable signal drop-out with fat saturation or opposed-phase imaging. They can appear mass-like or the affected kidney might retain its reniform shape. The imaging pattern of fat-poor AMLs differs from that of most renal cell carcinomas because renal cell carcinoma is generally heterogeneously hyperintense on T2-weighted images [38, 39]. Contrast agent does not typically help to differentiate fat-poor AMLs from renal cell carcinoma and thus it is not needed for abdominal imaging.

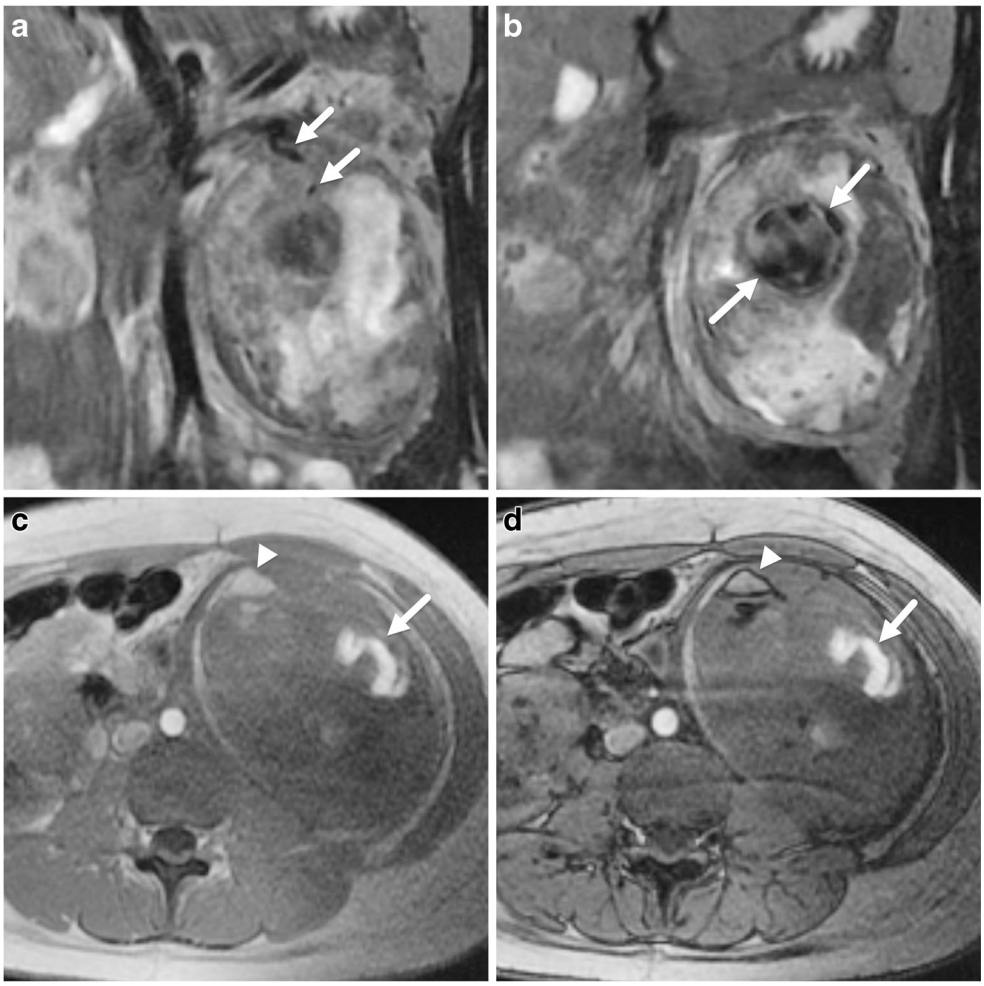

Fig. 3 Tuberous sclerosis complex and renal angiomyolipoma (AML) in a 15-year-old girl. **a** Coronal T1-weighted MR image focused on the left kidney shows a large AML with internal hemorrhage. A small vessel (*arrows*) feeds an intralesional aneurysm. **b** Coronal T1-weighted MR sequence shows the 3-cm aneurysm (*arrows*). **c** Axial T1-weighted MR image shows an area of hemorrhage (*arrow*) and fat (*arrowhead*) within the large AML. **d** Axial opposed-phase MR image at the same level shows signal dropout at the periphery of the fat-containing (*arrowhead*) portion of the lesion but not at the hemorrhage (*arrow*)

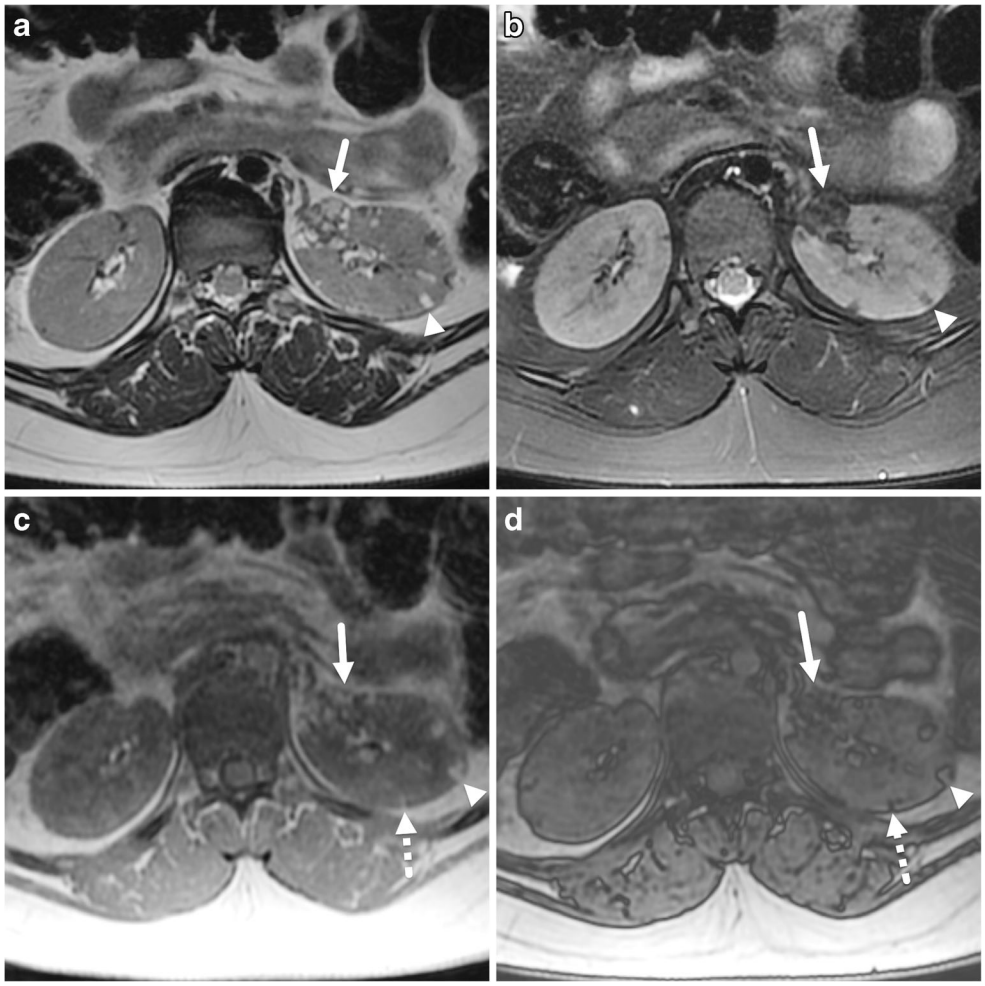

Fig. 4 Tuberous sclerosis complex and multiple angiomyolipomas (AMLs) in a 17-year-old girl. **a** Axial T1-weighted MR image shows multiple AMLs in the left kidney. The more anterior lesion (*arrow*) is larger and has more heterogeneous internal composition. The posterior lesion (*arrowhead*) is smaller and appears to be predominantly composed of fat. **b** Axial T2-weighted MR image with fat saturation shows signal suppression within both lesions described in (**a**). The more anterior lesion (*arrow*) has some internal signal because of its complexity. **c, d** Axial in-phase (**c**) and opposed-phase (**d**) MR images show the same lesions as described in (**a**) and (**b**) as well as a very small third lesion (*dashed arrow*). The largest lesion (*solid arrow*) has a heterogeneous appearance with mottled signal dropout because of its internal smooth muscle and small vessels. The intermediate-size lesion (*arrowhead*) has signal dropout at the periphery on the opposed-phase image from fat and soft-tissue sharing the same voxel. The smallest lesion (*dashed arrow*) has complete signal dropout on the opposed-phase image because of its small size and the fact that fat and soft tissue share all of the same voxels

AMLs have been shown to decrease in size and number with mTOR inhibitor therapy. However the lesions can return and increase in size if therapy is suspended [40].

Cysts

Renal cysts are another common finding in children with TSC, occurring in 17–47% of pediatric patients [41, 42]. Because of their frequency, multiple renal cysts are considered a minor feature in the clinical diagnosis of TSC. They are often seen in combination with AMLs and, like AMLs, cysts are commonly bilateral, multiple and of variable size [41–43]. Renal cysts can eventually lead to renal insufficiency or hypertension as they replace the renal parenchyma.

On MR imaging, the renal cysts can vary in size from a millimeter or less in diameter to several centimeters in diameter. Cysts are generally simple-appearing with a thin external rim and internal fluid signal intensity (Fig. 7). Occasionally a cyst has internal hemorrhage, making it appear hyperintense on T1-weighted images and hypointense on T2-weighted images. While contrast agent is not needed to diagnose renal cysts, if administered, cysts might display mild peripheral enhancement. A recent study has shown that small renal cysts can decrease in size and number after mTOR inhibitor therapy [18].

A small subset (1–9%) of people with TSC have multiple large renal cysts that completely or nearly completely

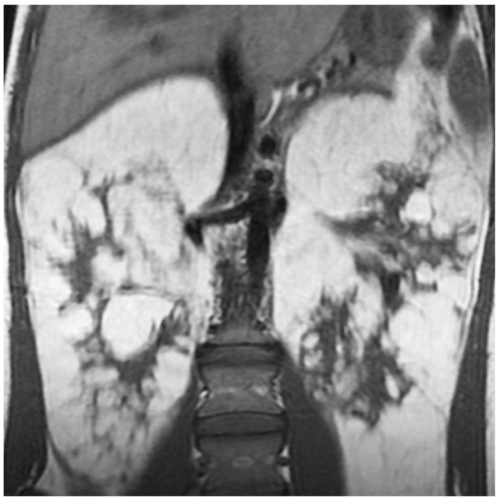

Fig. 5 Tuberous sclerosis complex diffuse infiltration of the kidneys with large angiomyolipomas (AMLs) in an 18-year-old woman. Coronal T1-weighted MR image shows enlargement and complete replacement of the kidneys with large AMLs. Even though the kidney is completely replaced by tumor, it maintains its reniform shape

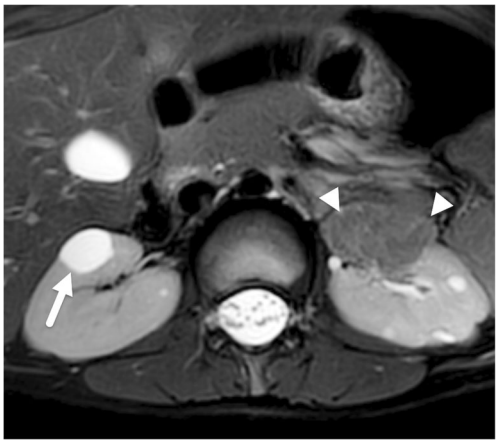

Fig. 7 Tuberous sclerosis complex, multiple renal cysts, and a fat-poor renal angiomyolipoma (AML) in a 7-year-old boy. Axial T2-weighted MR image with fat saturation shows multiple cysts in both kidneys. The largest cyst (*arrow*) is present in the right kidney. Each of the cysts is homogeneously hyperintense. In addition to the cysts, there is a fat-poor AML (*arrowheads*) arising from the anterior aspect of the left kidney

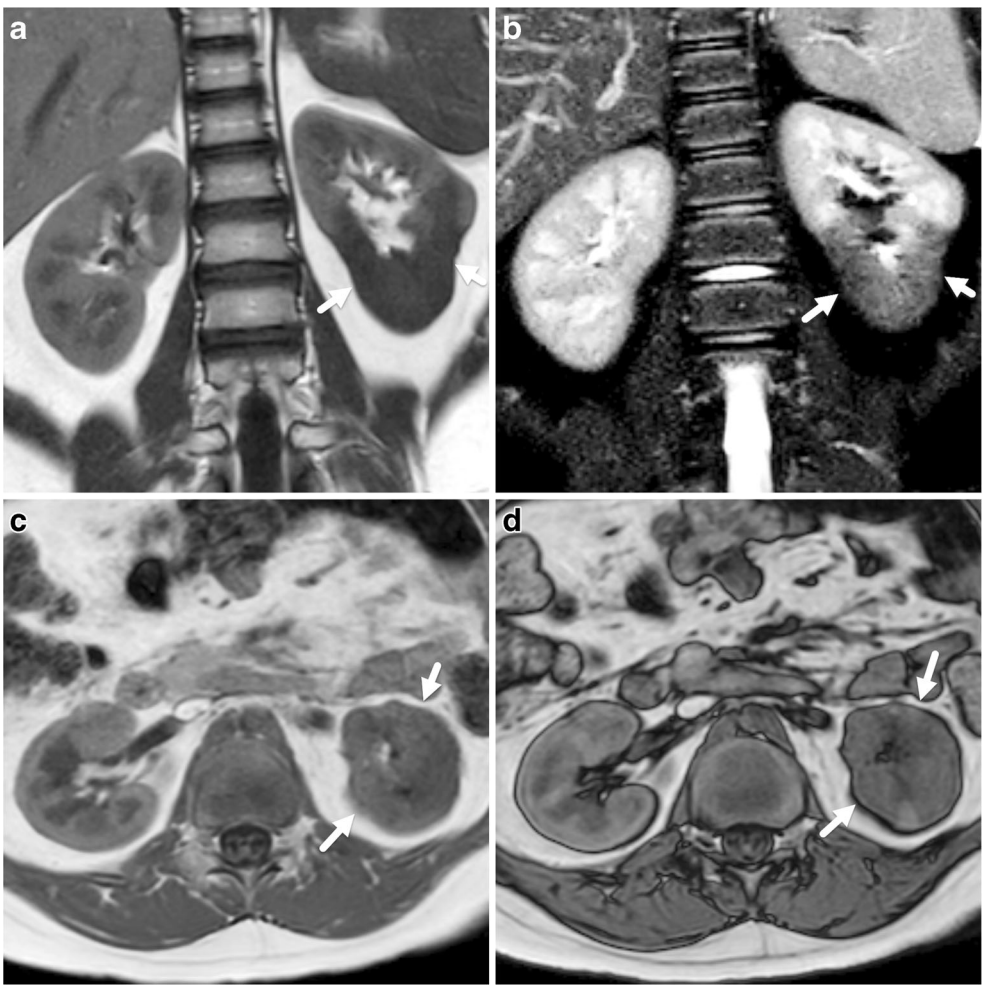

Fig. 6 Tuberous sclerosis complex and a fat-poor angiomyolipoma (AML) in an 11-year-old boy. **a, b** Coronal T1-weighted MR image (**a**) and coronal T2-weighted MR image with fat saturation (**b**) show a fat-poor AML (*arrows*) in the lower pole of the left kidney. The lesion maintains the normal reniform shape and has diffuse low signal compared to the remainder of the kidney on both imaging sequences. **c, d** Axial in-phase (**c**) and opposed-phase (**d**) images show the same lesion (*arrows*), which does not have signal drop-out on the opposed-phase image

replace the kidney, similar to the imaging appearance of autosomal-dominant polycystic kidney disease (ADPKD). This appearance occurs as a result of contiguous mutations in the *TSC2* gene and its neighbor on chromosome 16 that is responsible for ADPKD, the *PKD1* gene [34, 41, 42, 44, 45]. People with this so-called contiguous gene syndrome tend to present early in infancy or childhood with severe disease, resembling ADPKD at the time of diagnosis (Fig. 8).

Like AMLs, cysts can occur in other locations outside the kidneys. The most common location for extra-renal cysts is the liver [46]. Cysts have also been described in the pancreas and adrenal glands.

Renal cell carcinoma

The literature is not clear on whether children with TSC have an increased risk over the general population of developing renal cell carcinoma. A meta-analysis of all reported cases of renal cell carcinoma in TSC suggests there is not an increased risk [47]. Many reports describe the incidence of renal cell carcinoma in people with TSC to be between 2% and 4%, although a primary reference for this statement cannot be found. If the incidence of developing renal cell carcinoma in people with TSC is truly 2–4%, this would be similar to the 1.6–3.8% incidence of renal cell carcinoma in the general population [48]. Further complicating this question is the fact that the histological distinction of lipid-poor AMLs and renal cell carcinoma is known to be difficult.

While there is not a clear increased risk of renal cell carcinoma in children with TSC, there do appear to be differences in the renal cell carcinoma when present. First, people with TSC and renal cell carcinoma are younger than those with renal cell carcinoma in the general population [37, 49, 50]. In one study, people with TSC and renal cell carcinoma were diagnosed at a mean age of 28 years [51]. This is 36 years younger than the current mean age of diagnosis (64 years) of renal cell carcinoma in the general population [48]. In addition to being diagnosed at a younger age, people with TSC and renal cell carcinoma tend to have less aggressive disease [7, 52, 53].

Renal cell carcinomas are generally heterogeneously hyperintense on T2-W MRI and demonstrate other findings of malignancy, including restricted diffusion and enhancement [38, 39, 51, 54, 55]. Unfortunately, these characteristics are not unique because fat-poor AMLs can also show restricted diffusion and enhancement. Recent research has suggested that there is a significant difference in the apparent diffusion coefficient (ADC) value and diffusion coefficient between clear cell renal cell carcinomas and fat-poor AMLs, potentially allowing for distinction [56, 57].

Splenic hamartomas

Hamartomas of the spleen are rare in TSC [58]. If the lesion is large enough, it can cause abdominal pain [58]. On MRI (Fig. 9), splenic hamartomas can be difficult to identify because they are often isointense to the background spleen on both T1- and T2-weighted images. Larger lesions deform the splenic capsule and can be either mildly hypointense or mildly

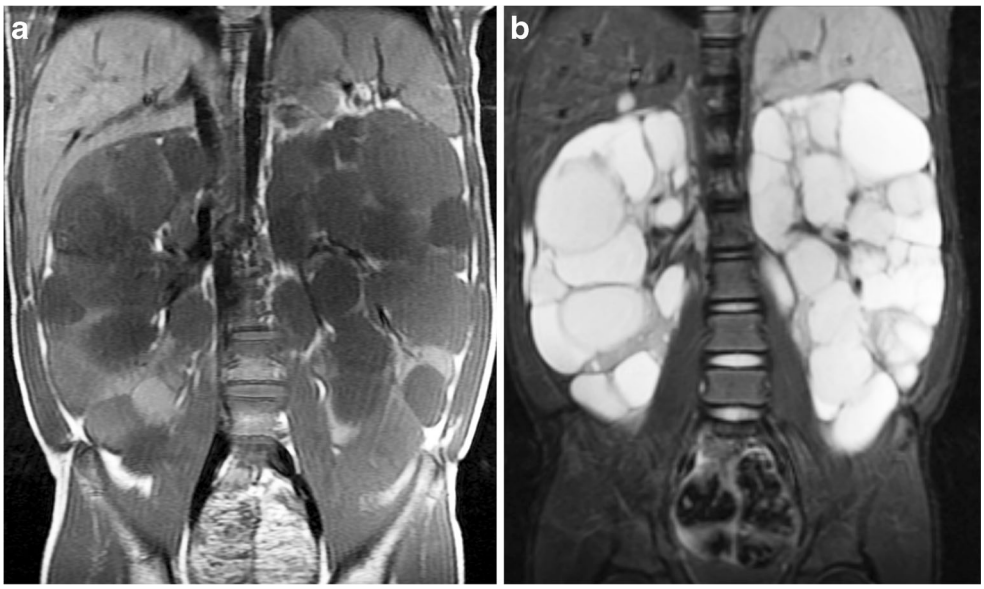

Fig. 8 Tuberous sclerosis complex and renal and hepatic cysts in a 7-year-old boy. **a, b** Coronal T1-weighted (**a**) and T2-weighted (**b**) MR images with fat saturation show near-complete replacement of the kidneys with innumerable cysts. The cysts have variable signal intensity because of internal hemorrhage and protein

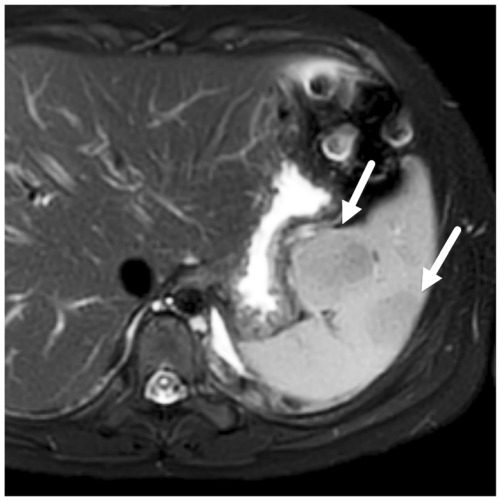

Fig. 9 Tuberous sclerosis complex and splenic hamartomas in an 11-year-old girl. Axial T2-weighted MR image with fat saturation shows two slightly hypointense splenic hamartomas (*arrows*). The anterior lesion deforms the splenic capsule

hyperintense on T2-weighted images and hypointense on T1-weighted images. If contrast agent is administered, splenic hamartomas can show diffuse enhancement because of increased vascularity [59–62]. Larger lesions can also have scattered foci of low signal on T1- and T2-weighted images because of fibrous tissue. Occasionally the fibrous tissue is more extensive and appears as a hypointense central scar [7].

Pancreatic neuroendocrine tumors

Prior to the era of routine cross-sectional imaging, pancreatic neuroendocrine tumors were thought to have a rare association with TSC. More recently an increased incidence of pancreatic neuroendocrine tumors associated with TSC has been reported of 4–9% [63–66]. Most of the tumors are reported to be non-functioning and are found incidentally on imaging. Many pancreatic lesions do not have pathological proof because of the patient's higher surgical risk as well as the lesion's slow growth and asymptomatic nature.

On MRI, pancreatic neuroendocrine tumors associated with TSC are typically 4 mm to 6 cm in diameter with well-circumscribed margins (Fig. 10) [65, 66]. They are more commonly located in the pancreatic body/tail. The tumors are hypointense to the pancreatic parenchyma on T1-weighted images and hyperintense on T2-weighted images. Pancreatic neuroendocrine tumors can be differentiated from pancreatic AMLs by their lack of intralesional fat and their increased T2-weighted signal. Lesions sometimes restrict diffusion.

Perivascular epithelioid tumors

Perivascular epithelioid tumors (PEComas) are mesenchymal tumors composed of unusual perivascular epithelioid cells (PECs), without a normal counterpart. The tumor cells coexpress smooth muscle and melanocytic markers [24, 26, 67–70]. Genetically, PEComas are most often related to loss of function mutations in TSC genes and can occur sporadically in people with TSC [26, 69, 71].

PEComas are thought to be part of a family of tumors that includes AMLs, clear cell sugar tumor of the lung, and LAM [24, 67]. Generally PEComas are low-grade tumors with a benign clinical course. However a small subset of PEComas demonstrates malignant behavior with local recurrence and hematogenous spread [72, 73]. These can occur in various anatomical sites including the skin, soft tissues, bone and viscera.

Fig. 10 Tuberous sclerosis complex and pancreatic neuroendocrine tumor in a 15-year-old boy. **a–c** Axial T1-weighted (**a**), T2-weighted with fat saturation (**b**) and axial T1-weighted post-contrast (**c**) MR images show a lesion (*arrow*) in the head of the pancreas. The lesion is hypointense on T1-W pre-contrast imaging (**a**), hyperintense on T2-weighting (**b**) and enhances after administration of contrast agent (**c**). The lesion was not biopsied but was presumed to be a neuroendocrine tumor given the child's underlying diagnosis, the lack of intralesional fat (not shown) and the hyperintense T2 signal

TSC is much less strongly associated with PEComas outside of AMLs and LAM [71]. However case reports of pancreatic PEComa [72], uterine PEComa [74] and peritoneal PEComa [73] have been reported.

On MRI, PEComas are hyperintense compared to muscle on T2-weighted images (Fig. 11). The lesions are typically vascular with avid enhancement [75]. As the lesions grow, there can be central areas of necrosis that do not enhance on post-contrast imaging. Large tumor vessels can often be seen adjacent to the tumors. Hematogenous spread can occur, causing lung, liver and bone metastases [72, 73].

Aneurysms/TSC-associated arteriopathy

Vascular aneurysms, independent from the aneurysms occurring within AMLs, are an uncommon complication of TSC and can affect vessels of any size. Aneurysms of the aorta and cerebral vessels in TSC can occur at a very early age [76–79]. Aneurysms affecting the iliac/femoral and pulmonary arteries have also been reported [76, 77, 80–86]. A 2001 review of aortic aneurysms found 15 total reports of aortic aneurysms associated with TSC, 12 abdominal and 4 thoracic (1 patient had both), 5 of which presented with rupture [77]. Given their low incidence, screening for vascular aneurysms was not recommended by the 2012 consensus conference. Once detected, regular screening is prudent because a rapid increase in size leading to rupture and sudden death has been reported [76, 78, 87].

The histopathological cause of arteriopathy in TSC is unknown, but pathological specimens have demonstrated intimal fibroplasia, medial atrophy and focal medial disruption contributing to abnormal physiology of the arterial walls [77]. On imaging, the aneurysms can appear fusiform or saccular (Fig. 12).

Vascular stenosis can also occur in people with TSC, including case reports of mid-aortic syndrome with bilateral renal artery stenosis and celiac artery stenosis [79, 88, 89].

Lymphangioleiomyomatosis

Lymphangioleiomyomatosis (LAM) is a multi-system disorder that almost exclusively affects females of reproductive and middle-age in either its sporadic (S-LAM) or TSC-related form (TSC-LAM) [90–92]. LAM is characterized by cystic lung destruction, cystic fluid-

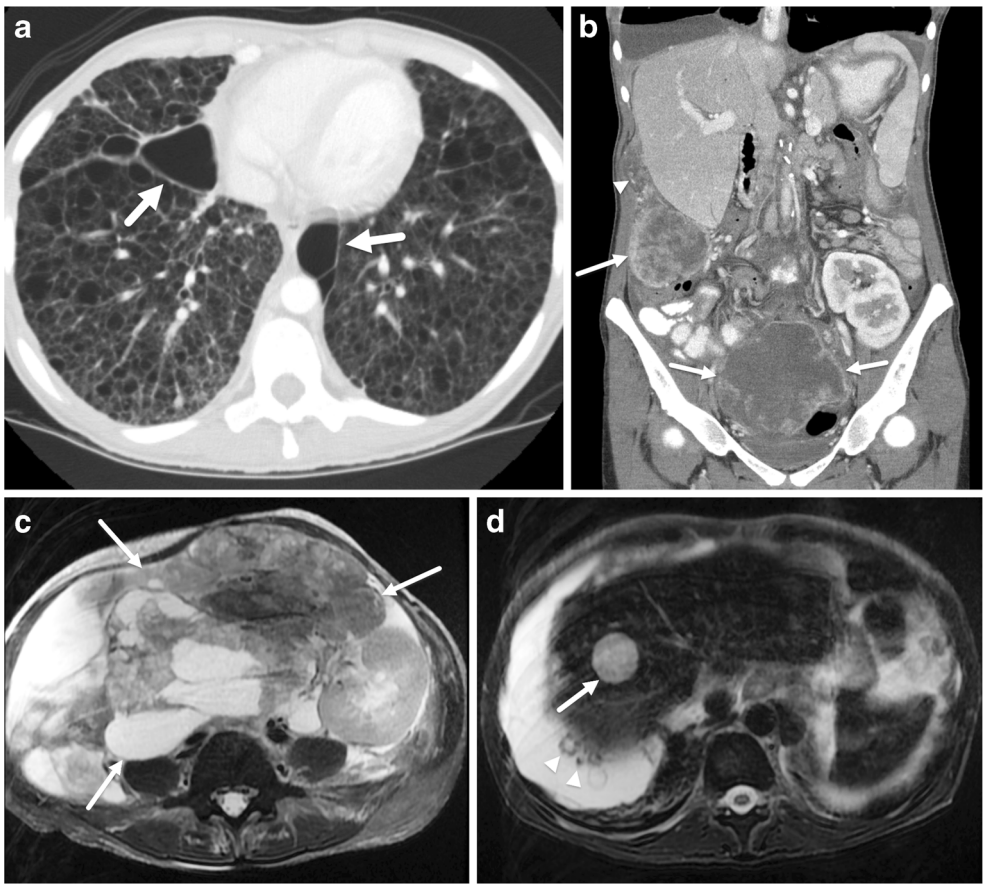

Fig. 11 Tuberous sclerosis complex and perivascular epithelioid tumors (PEComa) and advanced lymphangioleiomyomatosis in a 35-year-old woman. **a** Axial CT image shows extensive cystic change of the lungs with small, bilateral loculated pneumothoraces (*arrows*). **b** Coronal contrast-enhanced CT shows a multifocal peritoneal PEComa (*arrows*). The masses display peripheral enhancement and central necrosis. There are large vessels (*arrowhead*) adjacent to the right margin of the liver, superior to the upper abdominal mass. **c** Axial T2-W MR image shows the large heterogeneous PEComa (*arrows*). The mass has both cystic and solid components. **d** Axial T2-W MR image of the liver shows an intrahepatic metastasis (*arrow*) and large vessels (*arrowheads*) at the periphery of the liver

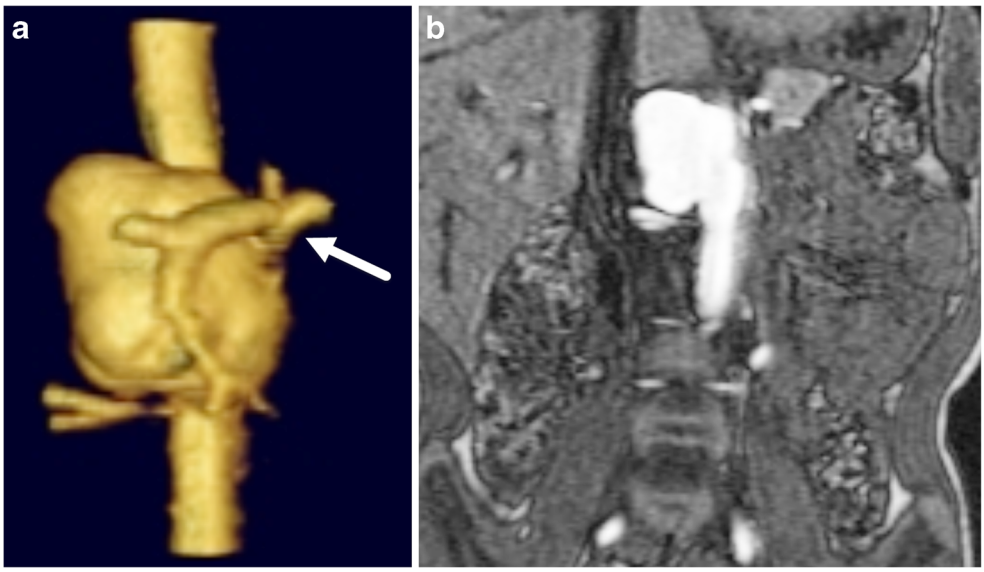

Fig. 12 Tuberous sclerosis complex and a saccular abdominal aortic aneurysm in a 5-year-old boy. **a** Three-dimensional volumetric reconstruction of the abdominal aorta shows a saccular aneurysm at the level of the origin of the celiac axis (*arrow*). **b** Coronal source magnetic resonance angiography image obtained after administration of a gadolinium-based contrast agent shows the saccular abdominal aortic aneurysm

filled masses involving their lymphatics, and abdominal angiomyolipomas [92–95]. LAM is a major feature as part of the clinical diagnostic criteria of TSC. However, because S-LAM is also associated with AMLs, people with LAM and AMLs without other major or minor features are not considered to have TSC [1].

LAM is the most common pulmonary manifestation of TSC, occurring in 26–49% of patients [46, 93, 96–99]. LAM reflects disordered, immature-appearing smooth muscle proliferation in a lymphatic distribution around the airways, blood vessels and lymphatic vessels [24, 69, 90, 100]. LAM cells infiltrate bronchioli of distal airways, leading to airway obstruction, resulting in air-trapping and alveolar disruption, which in turn leads to cystic change and spontaneous pneumothorax [91, 100, 101]. Similarly, around the pulmonary venules, smooth muscle proliferation causes obstruction in the form of venous congestion and dilation, resulting in hemoptysis and hemosiderosis. While around the arterioles, it leads to pulmonary hypertension and right heart failure, and around the lymphatics, it leads to chylothorax [91, 100]. Thus, pulmonary manifestations of LAM include dyspnea, recurrent spontaneous, chylous pleural effusion and hemoptysis. Clinically, people with TSC-LAM show impairment in lung function studies more commonly than people with TSC but without LAM [96].

If LAM has not been diagnosed, people with TSC should be screened by CT every 5–10 years. At the onset of a LAM diagnosis, imaging should be more frequent at 2–3 years, and with advanced disease, screening might be needed as often as every 3–6 months to aid in clinical decision-making [20].

Radiologically, LAM manifests on chest radiograph with diffuse interstitial infiltrates, cystic or bullous changes, hyperinflation or pneumothorax [91]. CT scan has a classic appearance with numerous homogeneous and well-defined cysts with thin walls, seen in all lobes of the lungs (Figs. 11 and 13) [91, 97, 102–104]. The European Respiratory Society guidelines for diagnosis of LAM include the following criteria on CT: “multiple (>10) thin-walled round well-defined air-filled cysts with preserved or increased lung volume with no other significant pulmonary involvement, specifically no interstitial lung disease with the exception of possible features of multifocal micronodular pneumocyte hyperplasia in patients with TSC” [93]. Quantitative CT grading has been shown to correlate with physiological measurements of lung function [105]. MRI has not been commonly used to diagnose LAM, although one report demonstrates visibility of classic cystic change on MR [106].

Fig. 13 Tuberous sclerosis complex and lymphangioleiomyomatosis (LAM) in an 18-year-old woman. Axial CT of the lungs shows multiple small cysts (*arrow*) at the lung bases typical of the early findings of LAM

Fig. 14 Tuberous sclerosis complex and a large spontaneous pneumothorax and multifocal micronodular pneumocyte hyperplasia (MMPH) in a 17-year-old boy. Axial maximum-intensity projection CT image shows multiple pulmonary nodules (*arrows*) typical of MMPH. In addition, there is a large left-side pneumothorax

Multifocal micronodular pneumocyte hyperplasia

Micronodular hyperplasia of type II pneumocytes was initially described as a new lung lesion associated with TSC in 1991 and subsequently named multifocal micronodular pneumocyte hyperplasia (MMPH) in 1995 [90, 107, 108]. MMPH involves both pneumocyte hyperplasia and the ingrowth of proliferating epithelial cells into the alveolar walls [90]. After LAM, MMPH is the next most frequent pulmonary manifestation of TSC [104]. MMPH has been reported in both males and females with TSC and females with sporadic-LAM. The frequency of nodules seen on CT, presumably related to MMPH, is approximately 3–36% in people with LAM and higher in those with TSC-LAM (12–64%) and 43–50% in people with TSC [96, 97, 99, 103, 109]. Clinically, people with TSC and MMPH can have no or mild symptoms and in one study did not differ from TSC patients without pulmonary manifestations in terms of clinical features or lung function studies [96, 110].

MMPH is characterized on CT as multiple small solid or ground-glass nodules (1–10 mm), scattered throughout the lungs in a random or miliary distribution (Fig. 14) [97, 102, 111, 112]. This nonspecific pattern can be challenging to distinguish from granulomatous, metastatic or infectious nodules, and a history of TSC or findings of LAM is helpful for diagnosis. Because both fat-poor AMLs and MMPH are relatively common in the setting of TSC, small pulmonary nodules should not be considered as definitive evidence of renal cell carcinoma with metastatic disease. MMPH is uncommonly seen on MR imaging because of the small nodule size. When visible, the nodules are of intermediate signal intensity on T1- and T2-weighted images.

Cardiac rhabdomyoma

Cardiac rhabdomyomas are benign tumors of the heart. They typically occur in children younger than 2 years and represent the first imaging manifestation of TSC in 56% of patients [113]. Frequently these tumors are diagnosed prenatally and strongly suggest a diagnosis of TSC, with approximately 50–80% of people diagnosed with rhabdomyomas having TSC [112–117]. Generally rhabdomyomas are asymptomatic, but they can cause heart murmurs, arrhythmias, outflow obstruction or heart failure [114, 116]. While the tumors can vary in size from 2 mm to 20 mm at the time of diagnosis [114], they typically regress spontaneously by 2 years of age (Fig. 15). However, because some rhabdomyomas have been shown to progress in size, follow-up imaging with echocardiography is recommended to document resolution [114, 116].

Rhabdomyomas can be single or multiple and can be located in any chamber, although they are more common in the ventricles (Figs. 15 and 16) [114, 116, 118]. The tumors are homogeneous on all sequences and are typically mildly hyperintense compared to the myocardium on T2-weighted imaging, hypoenhancing compared to the myocardium on first-pass perfusion (vs. minimally hyperintense), and isointense on delayed enhancement sequences [119].

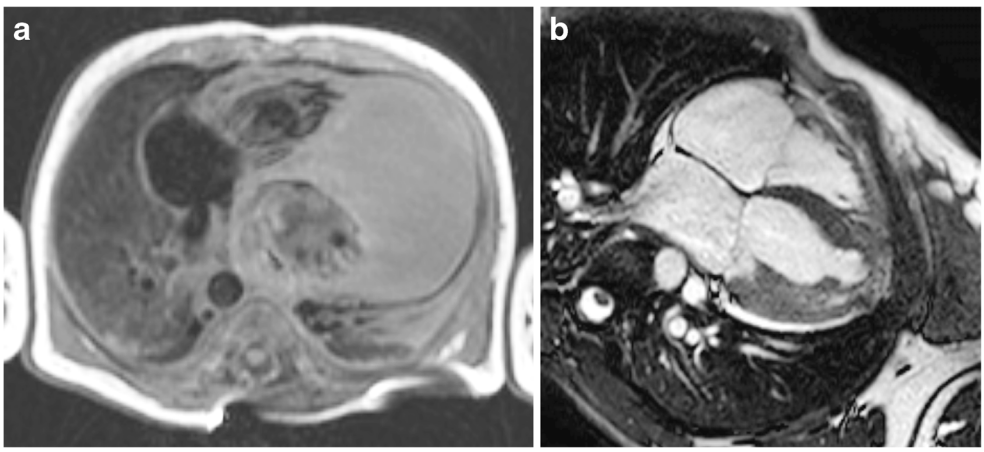

Fig. 15 Tuberous sclerosis complex and a cardiac rhabdomyoma in a male patient. **a** Axial black-blood MR image at 3 days old shows a large cardiac mass arising from the interventricular septum. **b** Four-chamber white-blood image of the heart 21 years later shows that the mass has completely resolved

Fig. 16 Tuberous sclerosis complex and a cardiac rhabdomyoma in a 4-month-old boy. Axial T2-weighted MR image shows a hyperintense mass (*arrow*) arising from the right atrial wall

Fig. 18 Tuberous sclerosis complex and lymphedema in a 15-month-old boy. Coronal T2-weighted MR image with fat saturation shows diffuse enlargement and subcutaneous fluid signal in the left lower extremity

Myocardial fat foci

Incidental detection of fat-containing cardiac lesions is relatively common in people with TSC, reported to occur in 35–64% of people screened for other purposes [120–122]. Lesions are typically well-circumscribed and follow fat signal on all imaging sequences. The foci are commonly located in the interventricular septum or left ventricular wall (Fig. 17). Generally lesions are small, but they are rarely large enough to cause mass effect. Occasionally, fat can appear to completely replace the myocardium. A limited number of myocardial fat foci has been examined at histopathology and have been shown to be either AMLs or areas of mature fat cells without invasion, an associated capsule, or fibrosis. This appearance is in contrast to arrhythmogenic right ventricular dysplasia or inherited myopathies (which are associated with fibrosis), intracardiac lipomas (which have a capsule) and liposarcoma (which is invasive) [120, 123]. Lesions are easily differentiated from the classic subendocardial apical fatty lesion, consistent with old infarct based on location [121].

Lymphatic malformation

Congenital or primary lymphedema and lymphatic malformations are extremely rare in the setting of TSC and are characterized by a buildup of fluid in tissues related to developmental abnormalities in the lymphatic system [124]. A retrospective review of people with TSC demonstrated an incidence of lymphedema in 3.7% (10/268) [125]. In addition to the cystic fluid-filled masses involving the lymphatics in people with LAM, lymphedema is associated with TSC-LAM at a reportedly higher incidence than in the non-LAM TSC population. In one retrospective review, 32% (8/25) of people

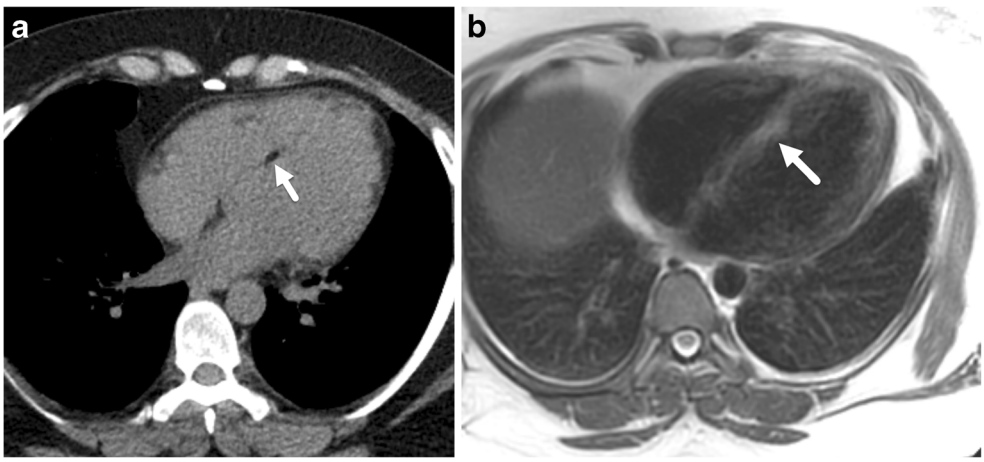

Fig. 17 Tuberous sclerosis complex and a focus of myocardial fat in an 18-year-old woman. **a** Axial CT image shows a focus of hypointense fat (*arrow*) within the interventricular septum. **b** Axial T2-weighted MR image shows the same lesion (*arrow*) to have increased signal similar to the subcutaneous fat on the initial image of an abdominal MRI

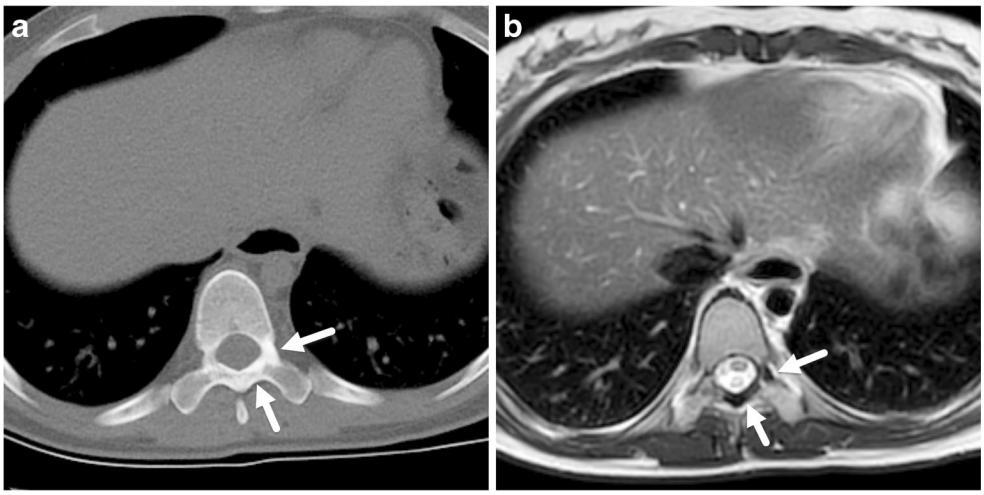

Fig. 19 Tuberous sclerosis complex and a sclerotic focus in the vertebral body in an 18-year-old woman. **a**, **b** Axial CT (**a**) and axial T1-weighted MR (**b**) images of a lower thoracic vertebral body show sclerosis in the left pars and lamina (*arrows*)

with TSC-LAM had lymphedema while none of the 203 patients with S-LAM had this finding [126]. Generally, the diagnosis is made clinically; however occasionally imaging is performed (Fig. 18) [125, 127–132]. These lesions have been reported to improve with mTOR inhibitor therapy [133, 134].

Bone islands/skeletal findings

Osseous findings that are associated with TSC were initially described in 1952 by Holt and Dickerson [135] and include "scattered sclerotic plaques, cyst-like areas of bone destruction in the phalanges, and wavy periosteal new bone formation along the metatarsals and metacarpals."

A retrospective review of abdominal MRI scans in 70 pediatric patients with TSC found sclerotic bone lesions in 73% of the children [136]. Multiple sclerotic lesions were common and most were located in the posterior elements of the vertebrae (Fig. 19). Because this study was limited to abdominal MRIs, the true prevalence and distribution of sclerotic bone lesions in children with TSC remains incompletely defined. On MRI, sclerotic bone lesions were hypointense on both T1- and T2-weighted images and do not enhance. Prior diagnostic criteria for TSC included bone cysts as a minor feature (Fig. 20), but this was removed from the more recent criteria for lack of specificity and rarity of diagnosis in the absence of more common TSC-associated findings [1, 3]. Similarly, wavy periosteal new bone formation is nonspecific but has been reported in cases of TSC [137].

Conclusion

In addition to the classic neurologic and dermatologic findings of tuberous sclerosis complex, multiple organs are involved in the chest and abdomen. Baseline and ongoing surveillance imaging is recommended for both the chest (by CT) and abdomen (by MRI). Many of the rarer associations discussed here are not common enough to warrant surveillance imaging in all children but should be recognized in children with clinical symptoms or in those with TSC otherwise undergoing

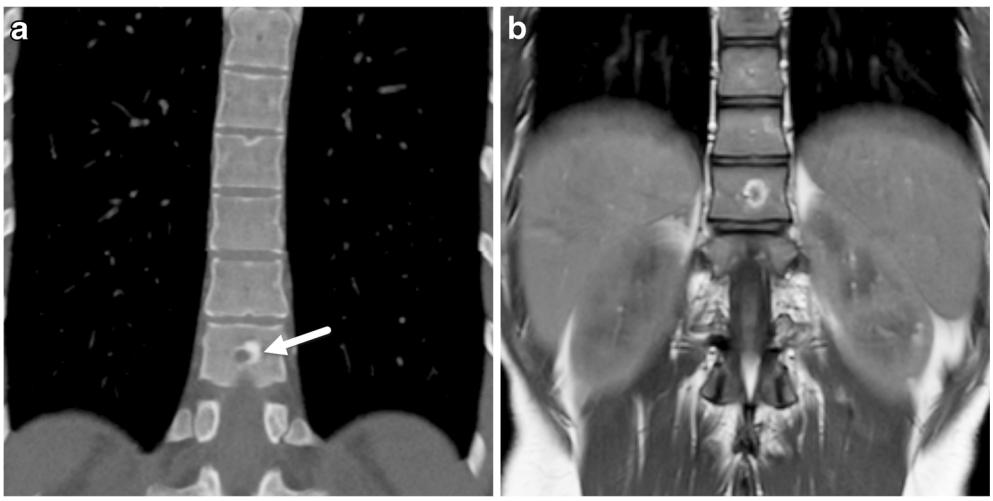

Fig. 20 Tuberous sclerosis complex and a mixed cystic and sclerotic bone lesion in an 18-year-old woman. **a** Coronal CT image of the spine shows a mixed cystic and sclerotic bone lesion (*arrow*) of a lower thoracic vertebral body. **b** Coronal T1-weighted MR image shows the same lesion has a peripheral area of increased signal and a central area of decreased signal when compared to the remainder of the vertebral body

screening. New advances in treatment with mTOR inhibitors are leading to exciting new possibilities in disease management and are likely to lead to increased survival and reinforce the need for ongoing surveillance imaging.

Compliance with ethical standards

Conflicts of interest Drs Franz and Krueger declared potential conflicts of interest.

References

1. Northrup H, Krueger DA, International Tuberous Sclerosis Complex Consensus Group (2013) Tuberous sclerosis complex diagnostic criteria update: recommendations of the 2012 International Tuberous Sclerosis Complex Consensus Conference. Pediatr Neurol 49:243–254
2. Caban C, Khan N, Hasbani DM, Crino PB (2017) Genetics of tuberous sclerosis complex: implications for clinical practice. Appl Clin Genet 10:1–8
3. Roach ES, Gomez MR, Northrup H (1998) Tuberous sclerosis complex consensus conference: revised clinical diagnostic criteria. J Child Neurol 13:624–628
4. O'Callaghan FJ, Shiell AW, Osborne JP, Martyn CN (1998) Prevalence of tuberous sclerosis estimated by capture-recapture analysis. Lancet 351:1490
5. Sampson JR, Scahill SJ, Stephenson JB et al (1989) Genetic aspects of tuberous sclerosis in the west of Scotland. J Med Genet 26:28–31
6. Randle SC (2017) Tuberous sclerosis complex: a review. Pediatr Ann 46:e166–e171
7. Manoukian SB, Kowal DJ (2015) Comprehensive imaging manifestations of tuberous sclerosis. AJR Am J Roentgenol 204: 933–943
8. Au KS, Williams AT, Roach ES et al (2007) Genotype/phenotype correlation in 325 individuals referred for a diagnosis of tuberous sclerosis complex in the United States. Genet Med 9:88–100
9. Webb DW, Clarke A, Fryer A, Osborne JP (1996) The cutaneous features of tuberous sclerosis: a population study. Br J Dermatol 135:1–5
10. Jóźwiak S, Schwartz RA, Janniger CK et al (1998) Skin lesions in children with tuberous sclerosis complex: their prevalence, natural course, and diagnostic significance. Int J Dermatol 37:911–917
11. Curatolo P, Bombardieri R, Jozwiak S (2008) Tuberous sclerosis. Lancet 372:657–668
12. Curatolo P, Moavero R, Roberto D, Graziola F (2015) Genotype/phenotype correlations in tuberous sclerosis complex. Semin Pediatr Neurol 22:259–273
13. Franz DN, Belousova E, Sparagana S et al (2013) Efficacy and safety of everolimus for subependymal giant cell astrocytomas associated with tuberous sclerosis complex (EXIST-1): a multicentre, randomised, placebo-controlled phase 3 trial. Lancet 381:125–132
14. Bissler JJ, Kingswood JC, Radzikowska E et al (2013) Everolimus for angiomyolipoma associated with tuberous sclerosis complex or sporadic lymphangioleiomyomatosis (EXIST-2): a multicentre, randomised, double-blind, placebo-controlled trial. Lancet 381: 817–824
15. Krueger DA, Wilfong AA, Holland-Bouley K et al (2013) Everolimus treatment of refractory epilepsy in tuberous sclerosis complex. Ann Neurol 74:679–687
16. Capal JK, Franz DN (2016) Profile of everolimus in the treatment of tuberous sclerosis complex: an evidence-based review of its place in therapy. Neuropsychiatr Dis Treat 12:2165–2172
17. French JA, Lawson JA, Yapici Z et al (2016) Adjunctive everolimus therapy for treatment-resistant focal-onset seizures associated with tuberous sclerosis (EXIST-3): a phase 3, randomised, double-blind, placebo-controlled study. Lancet 388:2153–2163
18. Siroky BJ, Towbin AJ, Trout AT et al (2017) Improvement in renal cystic disease of tuberous sclerosis complex after treatment with mammalian target of rapamycin inhibitor. J Pediatr 187:318–322.e2
19. Koenig MK, Hebert AA, Roberson J et al (2012) Topical rapamycin therapy to alleviate the cutaneous manifestations of tuberous sclerosis complex: a double-blind, randomized, controlled trial to evaluate the safety and efficacy of topically applied rapamycin. Drugs R D 12:121–126
20. Krueger DA, Northrup H, International Tuberous Sclerosis Complex Consensus Group (2013) Tuberous sclerosis complex surveillance and management: recommendations of the 2012 International Tuberous Sclerosis Complex Consensus Conference. Pediatr Neurol 49:255–265
21. Halpenny D, Snow A, McNeill G, Torreggiani WC (2010) The radiological diagnosis and treatment of renal angiomyolipoma — current status. Clin Radiol 65:99–108
22. Lopes Vendrami C, Parada Villavicencio C, DeJulio TJ et al (2017) Differentiation of solid renal tumors with multiparametric MR imaging. Radiographics 37:2026–2042
23. Lienert AR, Nicol D (2012) Renal angiomyolipoma. BJU Int 110 Suppl 4:25–27
24. Thway K, Fisher C (2015) PEComa: morphology and genetics of a complex tumor family. Ann Diagn Pathol 19:359–368
25. Katabathina VS, Vikram R, Nagar AM et al (2010) Mesenchymal neoplasms of the kidney in adults: imaging spectrum with radiologic-pathologic correlation. Radiographics 30:1525–1540
26. Jinzaki M, Silverman SG, Akita H et al (2014) Renal angiomyolipoma: a radiological classification and update on recent developments in diagnosis and management. Abdom Imaging 39:588–604
27. Fricke BL, Donnelly LF, Casper KA, Bissler JJ (2004) Frequency and imaging appearance of hepatic angiomyolipomas in pediatric and adult patients with tuberous sclerosis. AJR Am J Roentgenol 182:1027–1030
28. Lu J, Xiong X-Z, Cheng N-S (2014) Education and imaging. Hepatobiliary and pancreatic: hepatic and renal angiomyolipomas associated with tuberous sclerosis complex. J Gastroenterol Hepatol 29:421
29. Asayama Y, Fukuya T, Honda H et al (1998) Chronic expanding hematoma of the spleen caused by angiomyolipoma in a patient with tuberous sclerosis. Abdom Imaging 23:527–530
30. Hulbert JC, Graf R (1983) Involvement of the spleen by renal angiomyolipoma: metastasis or multicentricity? J Urol 130: 328–329
31. Morita K, Shida Y, Shinozaki K et al (2012) Angiomyolipomas of the mediastinum and the lung. J Thorac Imaging 27:W21–W23
32. Bissler JJ, Kingswood JC (2004) Renal angiomyolipomata. Kidney Int 66:924–934
33. Yamakado K, Tanaka N, Nakagawa T et al (2002) Renal angiomyolipoma: relationships between tumor size, aneurysm formation, and rupture. Radiology 225:78–82
34. O'Callaghan FJ, Noakes MJ, Martyn CN, Osborne JP (2004) An epidemiological study of renal pathology in tuberous sclerosis complex. BJU Int 94:853–857
35. Ouzaid I, Autorino R, Fatica R et al (2014) Active surveillance for renal angiomyolipoma: outcomes and factors predictive of delayed intervention. BJU Int 114:412–417

36. Dickinson M, Ruckle H, Beaghler M, Hadley HR (1998) Renal angiomyolipoma: optimal treatment based on size and symptoms. Clin Nephrol 49:281–286
37. Amin S, Lux A, Calder N et al (2017) Causes of mortality in individuals with tuberous sclerosis complex. Dev Med Child Neurol 59:612–617
38. Ramamurthy NK, Moosavi B, McInnes MDF et al (2015) Multiparametric MRI of solid renal masses: pearls and pitfalls. Clin Radiol 70:304–316
39. Chung MS, Choi HJ, Kim M-H, Cho K-S (2014) Comparison of T2-weighted MRI with and without fat suppression for differentiating renal angiomyolipomas without visible fat from other renal tumors. AJR Am J Roentgenol 202:765–771
40. Bissler JJ, McCormack FX, Young LR et al (2008) Sirolimus for angiomyolipoma in tuberous sclerosis complex or lymphangioleiomyomatosis. N Engl J Med 358: 140–151
41. Casper KA, Donnelly LF, Chen B, Bissler JJ (2002) Tuberous sclerosis complex: renal imaging findings. Radiology 225:451–456
42. Ewalt DH, Sheffield E, Sparagana SP et al (1998) Renal lesion growth in children with tuberous sclerosis complex. J Urol 160: 141–145
43. Dillman JR, Trout AT, Smith EA, Towbin AJ (2017) Hereditary renal cystic disorders: imaging of the kidneys and beyond. Radiographics 37:924–946
44. Brook-Carter PT, Peral B, Ward CJ et al (1994) Deletion of the TSC2 and PKD1 genes associated with severe infantile polycystic kidney disease — a contiguous gene syndrome. Nat Genet 8:328–332
45. Back SJ, Andronikou S, Kilborn T et al (2015) Imaging features of tuberous sclerosis complex with autosomal-dominant polycystic kidney disease: a contiguous gene syndrome. Pediatr Radiol 45: 386–395
46. Black ME, Hedgire SS, Camposano S et al (2012) Hepatic manifestations of tuberous sclerosis complex: a genotypic and phenotypic analysis. Clin Genet 82:552–557
47. Tello R, Blickman JG, Buonomo C, Herrin J (1998) Meta analysis of the relationship between tuberous sclerosis complex and renal cell carcinoma. Eur J Radiol 27:131–138
48. National Cancer Institute (2014) Cancer stat facts: kidney and renal pelvis cancer. https://seer.cancer.gov/statfacts/html/kidrp.html. Accessed 12 Nov 2017
49. Rakowski SK, Winterkorn EB, Paul E et al (2006) Renal manifestations of tuberous sclerosis complex: incidence, prognosis, and predictive factors. Kidney Int 70:1777–1782
50. Lendvay TS, Broecker B, Smith EA (2002) Renal cell carcinoma in a 2-year-old child with tuberous sclerosis. J Urol 168:1131–1132
51. Washecka R, Hanna M (1991) Malignant renal tumors in tuberous sclerosis. Urology 37:340–343
52. Crino PB, Nathanson KL, Henske EP (2006) The tuberous sclerosis complex. N Engl J Med 355:1345–1356
53. Guo J, Tretiakova MS, Troxell ML et al (2014) Tuberous sclerosis-associated renal cell carcinoma: a clinicopathologic study of 57 separate carcinomas in 18 patients. Am J Surg Pathol 38:1457–1467
54. Yang P, Cornejo KM, Sadow PM et al (2014) Renal cell carcinoma in tuberous sclerosis complex. Am J Surg Pathol 38:895–909
55. Bjornsson J, Short MP, Kwiatkowski DJ, Henske EP (1996) Tuberous sclerosis-associated renal cell carcinoma. Clinical, pathological, and genetic features. Am J Pathol 149:1201–1208
56. Li H, Liang L, Li A et al (2017) Monoexponential, biexponential, and stretched exponential diffusion-weighted imaging models: quantitative biomarkers for differentiating renal clear cell carcinoma and minimal fat angiomyolipoma. J Magn Reson Imaging 46:240–247
57. Ding Y, Zeng M, Rao S et al (2016) Comparison of biexponential and monoexponential model of diffusion-weighted imaging for distinguishing between common renal cell carcinoma and fat poor angiomyolipoma. Korean J Radiol 17:853–863
58. Darden JW, Teeslink R, Parrish A (1975) Hamartoma of the spleen: a manifestation of tuberous sclerosis. Am Surg 41:564–566
59. Ramani M, Reinhold C, Semelka RC et al (1997) Splenic hemangiomas and hamartomas: MR imaging characteristics of 28 lesions. Radiology 202:166–172
60. Torres GM, Terry NL, Mergo PJ, Ros PR (1995) MR imaging of the spleen. Magn Reson Imaging Clin N Am 3:39–50
61. Paterson A, Frush DP, Donnelly LF et al (1999) A pattern-oriented approach to splenic imaging in infants and children. Radiographics 19:1465–1485
62. Wang J-H, Ma X-L, Ren F-Y et al (2013) Multi-modality imaging findings of splenic hamartoma: a report of nine cases and review of the literature. Abdom Imaging 38:154–162
63. Arva NC, Pappas JG, Bhatla T et al (2012) Well-differentiated pancreatic neuroendocrine carcinoma in tuberous sclerosis — case report and review of the literature. Am J Surg Pathol 36:149–153
64. Díaz Díaz D, Ibarrola C, Goméz Sanz R et al (2012) Neuroendocrine tumor of the pancreas in a patient with tuberous sclerosis: a case report and review of the literature. Int J Surg Pathol 20:390–395
65. Larson AM, Hedgire SS, Deshpande V et al (2012) Pancreatic neuroendocrine tumors in patients with tuberous sclerosis complex. Clin Genet 82:558–563
66. Koc G, Sugimoto S, Kuperman R et al (2017) Pancreatic tumors in children and young adults with tuberous sclerosis complex. Pediatr Radiol 47:39–45
67. Buehler D, Weisman P (2017) Soft tissue tumors of uncertain histogenesis: a review for dermatopathologists. Clin Lab Med 37:647–671
68. Fletcher CDM, Krishnan Unni K, Mertens F (2002) Pathology and genetics of tumours of soft tissue and bone. IARC, Lyon
69. Martignoni G, Pea M, Reghellin D et al (2008) PEComas: the past, the present and the future. Virchows Arch 452:119–132
70. Bonetti F, Pea M, Martignoni G, Zamboni G (1992) PEC and sugar. Am J Surg Pathol 16:307–308
71. Agaram NP, Sung Y-S, Zhang L et al (2015) Dichotomy of genetic abnormalities in PEComas with therapeutic implications. Am J Surg Pathol 39:813–825
72. Hartley CP, Kwiatkowski DJ, Hamieh L et al (2016) Pancreatic PEComa is a novel member of the family of tuberous sclerosis complex-associated tumors: case report and review of the literature. Virchows Arch 469:707–710
73. Okamoto S, Komura M, Terao Y et al (2017) Pneumothorax caused by cystic and nodular lung metastases from a malignant uterine perivascular epithelioid cell tumor (PEComa). Respir Med Case Rep 22:77–82
74. Starbuck KD, Drake RD, Budd GT, Rose PG (2016) Treatment of advanced malignant uterine perivascular epithelioid cell tumor with mTOR inhibitors: single-institution experience and review of the literature. Anticancer Res 36:6161–6164
75. Tan Y, Zhang H, Xiao E-H (2013) Perivascular epithelioid cell tumour: dynamic CT, MRI and clinicopathological characteristics — analysis of 32 cases and review of the literature. Clin Radiol 68: 555–561
76. Calcagni G, Gesualdo F, Tamisier D et al (2008) Arterial aneurysms and tuberous sclerosis: a classic but little known association. Pediatr Radiol 38:795–797

77. Jost CJ, Gloviczki P, Edwards WD et al (2001) Aortic aneurysms in children and young adults with tuberous sclerosis: report of two cases and review of the literature. J Vasc Surg 33:639–642
78. Arora A, Bansal K, Sureka B (2015) Vascular, gastrointestinal, and urogenital associations of tuberous sclerosis: classic but less known. AJR Am J Roentgenol 205:W566
79. Rolfes DB, Towbin R, Bove KE (1985) Vascular dysplasia in a child with tuberous sclerosis. Pediatr Pathol 3:359–373
80. Dunet V, Qanadli SD, Lazor R (2013) Beigelman-Aubry C (2013) multiple pulmonary artery aneurysms in tuberous sclerosis complex. BMJ Case Rep. https://doi.org/10.1136/bcr-2012-007911
81. Wong H, Hadi M, Khoury T et al (2006) Management of severe hypertension in a child with tuberous sclerosis-related major vascular abnormalities. J Hypertens 24:597–599
82. Kimura Y, Sugimura H, Toda M et al (2005) A case of a 2-year-old boy with tuberous sclerosis complicated with descending aortic aneurysm. Pediatr Int 47:224–226
83. Patiño Bahena E, Calderón-Colmenero J, Buendía A, Juanico A (2005) Giant aortic aneurysm and rhabdomyomas in infant with tuberous sclerosis (case report). Arch Cardiol Mex 75:448–450
84. Moon S-B, Shin W-Y, Park Y-J, Kim S-J (2009) An abdominal aortic aneurysm in an 8-month-old girl with tuberous sclerosis. Eur J Vasc Endovasc Surg 37:569–571
85. Carette M-F, Antoine M, Bazelly B et al (2006) Primary pulmonary artery aneurysm in tuberous sclerosis: CT, angiography and pathological study. Eur Radiol 16:2369–2370
86. Burrows NJ, Johnson SR (2004) Pulmonary artery aneurysm and tuberous sclerosis. Thorax 59:86
87. Hyman MH, Whittemore VH (2000) National Institutes of Health consensus conference: tuberous sclerosis complex. Arch Neurol 57:662–665
88. Salerno AE, Marsenic O, Meyers KEC et al (2010) Vascular involvement in tuberous sclerosis. Pediatr Nephrol 25:1555–1561
89. Flynn PM, Robinson MB, Stapleton FB et al (1984) Coarctation of the aorta and renal artery stenosis in tuberous sclerosis. Pediatr Radiol 14:337–339
90. Maruyama H, Ohbayashi C, Hino O et al (2001) Pathogenesis of multifocal micronodular pneumocyte hyperplasia and lymphangioleiomyomatosis in tuberous sclerosis and association with tuberous sclerosis genes TSC1 and TSC2. Pathol Int 51:585–594
91. Castro M, Shepherd CW, Gomez MR et al (1995) Pulmonary tuberous sclerosis. Chest 107:189–195
92. Taveira-DaSilva AM, Pacheco-Rodriguez G, Moss J (2010) The natural history of lymphangioleiomyomatosis: markers of severity, rate of progression and prognosis. Lymphat Res Biol 8:9–19
93. Johnson SR, Cordier JF, Lazor R et al (2010) European Respiratory Society guidelines for the diagnosis and management of lymphangioleiomyomatosis. Eur Respir J 35:14–26
94. Darling TN, Pacheco-Rodriguez G, Gorio A et al (2010) Lymphangioleiomyomatosis and TSC2−/− cells. Lymphat Res Biol 8:59–69
95. Glasgow CG, Taveira-DaSilva A, Pacheco-Rodriguez G et al (2009) Involvement of lymphatics in lymphangioleiomyomatosis. Lymphat Res Biol 7:221–228
96. Di Marco F, Terraneo S, Imeri G et al (2016) Women with TSC: relationship between clinical, lung function and radiological features in a genotyped population investigated for lymphangioleiomyomatosis. PLoS One 11:e0155331
97. Franz DN, Brody A, Meyer C et al (2001) Mutational and radiographic analysis of pulmonary disease consistent with lymphangioleiomyomatosis and micronodular pneumocyte hyperplasia in women with tuberous sclerosis. Am J Respir Crit Care Med 164:661–668
98. Costello LC, Hartman TE, Ryu JH (2000) High frequency of pulmonary lymphangioleiomyomatosis in women with tuberous sclerosis complex. Mayo Clin Proc 75:591–594
99. Moss J, Avila NA, Barnes PM et al (2001) Prevalence and clinical characteristics of lymphangioleiomyomatosis (LAM) in patients with tuberous sclerosis complex. Am J Respir Crit Care Med 164: 669–671
100. Taylor JR, Ryu J, Colby TV, Raffin TA (1990) Lymphangioleiomyomatosis. Clinical course in 32 patients. N Engl J Med 323:1254–1260
101. Hammes SR, Krymskaya VP (2013) Targeted approaches toward understanding and treating pulmonary lymphangioleiomyomatosis (LAM). Horm Cancer 4:70–77
102. Umeoka S, Koyama T, Miki Y et al (2008) Pictorial review of tuberous sclerosis in various organs. Radiographics 28:e32
103. Tobino K, Johkoh T, Fujimoto K et al (2015) Computed tomographic features of lymphangioleiomyomatosis: evaluation in 138 patients. Eur J Radiol 84:534–541
104. von Ranke FM, Zanetti G, e Silva JLP et al (2015) Tuberous sclerosis complex: state-of-the-art review with a focus on pulmonary involvement. Lung 193:619–627
105. Crausman RS, Lynch DA, Mortenson RL et al (1996) Quantitative CT predicts the severity of physiologic dysfunction in patients with lymphangioleiomyomatosis. Chest 109:131–137
106. King MA (1996) MR diagnosis of lymphangioleiomyomatosis: visibility of pulmonary cysts on spin-echo images. Magn Reson Imaging 14:361–363
107. Popper HH, Juettner-Smolle FM, Pongratz MG (1991) Micronodular hyperplasia of type II pneumocytes — a new lung lesion associated with tuberous sclerosis. Histopathology 18: 347–354
108. Guinee D, Singh R, Azumi N et al (1995) Multifocal micronodular pneumocyte hyperplasia: a distinctive pulmonary manifestation of tuberous sclerosis. Mod Pathol 8:902–906
109. Avila NA, Dwyer AJ, Rabel A, Moss J (2007) Sporadic lymphangioleiomyomatosis and tuberous sclerosis complex with lymphangioleiomyomatosis: comparison of CT features. Radiology 242:277–285
110. Taniguchi H, Abo H, Uchiyama A, Noto H (2016) Multifocal micronodular pneumocyte hyperplasia with tuberous sclerosis. Intern Med 55:3407–3408
111. Ristagno RL, Biddinger PW, Pina EM, Meyer CA (2005) Multifocal micronodular pneumocyte hyperplasia in tuberous sclerosis. AJR Am J Roentgenol 184:S37–S39
112. Kobashi Y, Sugiu T, Mouri K et al (2008) Multifocal micronodular pneumocyte hyperplasia associated with tuberous sclerosis: differentiation from multiple atypical adenomatous hyperplasia. Jpn J Clin Oncol 38:451–454
113. Datta AN, Hahn CD, Sahin M (2008) Clinical presentation and diagnosis of tuberous sclerosis complex in infancy. J Child Neurol 23:268–273
114. Beghetti M, Gow RM, Haney I et al (1997) Pediatric primary benign cardiac tumors: a 15-year review. Am Heart J 134: 1107–1114
115. Grebenc ML, Rosado de Christenson ML, Burke AP et al (2000) Primary cardiac and pericardial neoplasms: radiologic-pathologic correlation. Radiographics 20:1073–1103
116. Jóźwiak S, Kotulska K, Kasprzyk-Obara J et al (2006) Clinical and genotype studies of cardiac tumors in 154 patients with tuberous sclerosis complex. Pediatrics 118:e1146–e1151
117. Harding CO, Pagon RA (1990) Incidence of tuberous sclerosis in patients with cardiac rhabdomyoma. Am J Med Genet 37:443–446
118. Jóźwiak S, Kawalec W, Dłuzewska J et al (1994) Cardiac tumours in tuberous sclerosis: their incidence and course. Eur J Pediatr 153: 155–157

119. Beroukhim RS, Prakash A, Valsangiacomo Buechel ER et al (2011) Characterization of cardiac tumors in children by cardiovascular magnetic resonance imaging. J Am Coll Cardiol 58: 1044–1054
120. Shaaya EA, Hirshberg JS, Rabe OT et al (2013) Cardiac fat-containing lesions are common in tuberous sclerosis complex. Am J Med Genet A 161A:1662–1665
121. Adriaensen MEAPM, Schaefer-Prokop CM, Duyndam DAC et al (2009) Fatty foci in the myocardium in patients with tuberous sclerosis complex: common finding at CT. Radiology 253:359–363
122. Winterkorn EB, Dodd JD, Inglessis I et al (2007) Tuberous sclerosis complex and myocardial fat-containing lesions: a report of four cases. Clin Genet 71:371–373
123. Adriaensen MEAPM, van Oosterhout MFM, Feringa HHH et al (2011) Mature fat cells in the myocardium of patients with tuberous sclerosis complex. J Clin Pathol 64:244–245
124. Connell FC, Gordon K, Brice G et al (2013) The classification and diagnostic algorithm for primary lymphatic dysplasia: an update from 2010 to include molecular findings. Clin Genet 84:303–314
125. Geffrey AL, Shinnick JE, Staley BA et al (2014) Lymphedema in tuberous sclerosis complex. Am J Med Genet A 164A:1438–1442
126. Hoshika Y, Hamamoto T, Sato K et al (2013) Prevalence and clinical features of lymphedema in patients with lymphangioleiomyomatosis. Respir Med 107:1253–1259
127. Hirsch RJ, Silverberg NB, Laude T, Weinberg JM (1999) Tuberous sclerosis associated with congenital lymphedema. Pediatr Dermatol 16:407–408
128. Voudris KA, Skardoutsou A, Vagiakou EA (2003) Tuberous sclerosis and congenital lymphedema. Pediatr Dermatol 20:371–373
129. Lucas M, Andrade Y (2011) Congenital lymphedema with tuberous sclerosis and clinical Hirschsprung disease. Pediatr Dermatol 28:194–195
130. Sukulal K, Namboodiri N (2012) Congenital lymphedema: another unique and gender specific stigmata of tuberous sclerosis? Indian Pediatr 49:845
131. Cottafava F, Cosso D, Brida di Priò S et al (1986) A case of Bourneville's tuberous sclerosis with elephantiasis (caused by lymphedema) of the left leg. Minerva Pediatr 38:49–52
132. Prato G, Mancardi MM, Baglietto MG et al (2014) Congenital segmental lymphedema in tuberous sclerosis complex with associated subependymal giant cell astrocytomas treated with Mammalian target of rapamycin inhibitors. J Child Neurol 29: NP54–NP57
133. Pollack SF, Geffrey AL, Thiele EA, Shah U (2015) Primary intestinal lymphangiectasia treated with rapamycin in a child with tuberous sclerosis complex (TSC). Am J Med Genet A 167A:2209–2212
134. Adams DM, Trenor CC 3rd, Hammill AM et al (2016) Efficacy and safety of sirolimus in the treatment of complicated vascular anomalies. Pediatrics 137:e20153257
135. Holt JF, Dickerson WW (1952) The osseous lesions of tuberous sclerosis. Radiology 58:1–7
136. Boronat S, Barber I, Pargaonkar V et al (2016) Sclerotic bone lesions at abdominal magnetic resonance imaging in children with tuberous sclerosis complex. Pediatr Radiol 46:689–694
137. Jonard P, Lonneux M, Boland B et al (2001) Tc-99m HDP bone scan showing bone changes in a case of tuberous sclerosis or Bourneville's disease. Clin Nucl Med 26:50–52